Supporting information

Density functional study on the photocatalytic degradation of polycaprolactone by decatungstate anion in acetonitrile solution

Noriyuki Minezawa,[a] Kosuke Suzuki,[b] and Susumu Okazaki[a]

[a] *Department of Applied Materials Science, Graduate School of Frontier Sciences,*

The University of Tokyo, 5-1-5 Kashiwanoha, Chiba, 277-8589, Japan.

[b] *Department of Applied Chemistry, School of Engineering,*

*The University of Tokyo, 7-3-1 Hongo, Bunkyo-ku, Tokyo, 113-8656, Japan.*

Section S1. Selection of density functional

Using several density functionals, we examined the thermodynamics of γ-hydrogen abstraction reaction, W10* + PCL–H → H–W10• + PCL$_\gamma$•. Here, W10* is the lowest triplet state of photocatalyst. We considered the functionals from pure generalized gradient approximation (GGA) to range-separated hybrid meta-GGA: revPBE,[1] BLYP, TPSS,[2,3] TPSSh,[4] B3LYP, PBE0 (this work),[5] B97M-D3BJ,[6,7] ωB97X-D3BJ,[6,8] and ωB97M-D3BJ.[6,9] We performed the geometry optimization and subsequent single-point energy calculation for every functional. The atom-pairwise dispersion correction was applied using the Becke–Johnson damping scheme (D3BJ).[10,11] The default parameter set provided by ORCA program suite[12] was used as it is.

Figure S1 shows the energy and Gibbs free energy of reaction at 298.15 K. Due to the lack of experimental and accurate computational data, there was no criteria for selecting the most appropriate functional. A through benchmark study using a total of 200 functionals and 5,000 data points shows that ωB97M-V range-separated hybrid meta-GGA is considered as most promising functional.[13] The reaction energy of −28.5 kcal/mol qualitatively reproduces the value by ωB97M-D3BJ result (−30.0 kcal/mol). Pure functionals tend to underestimate the exothermicity except

B97M-D3BJ. The reaction is slightly more exothermic as a mixing weight of Hartree–Fock exchange increases for the series of hybrid functionals. The same trends hold true for the Gibbs free energy of reaction.

(a)
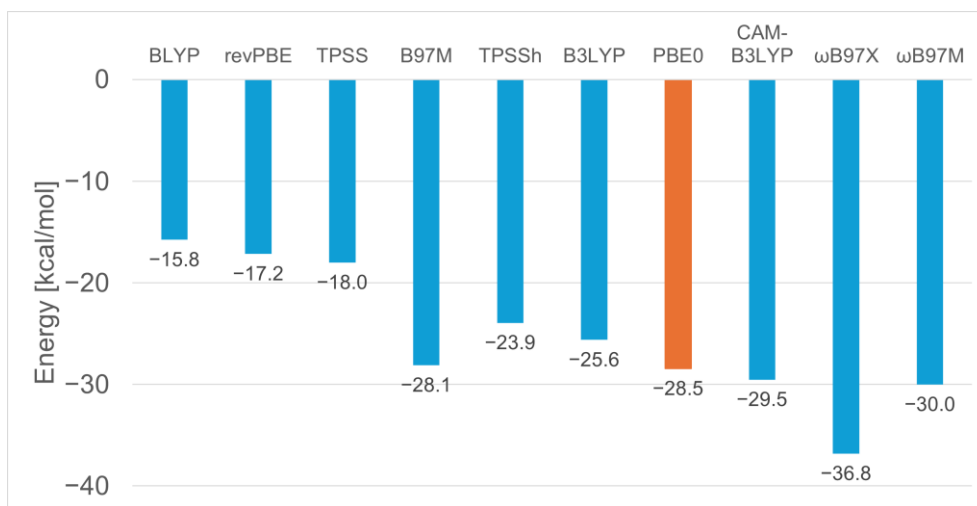
(b)
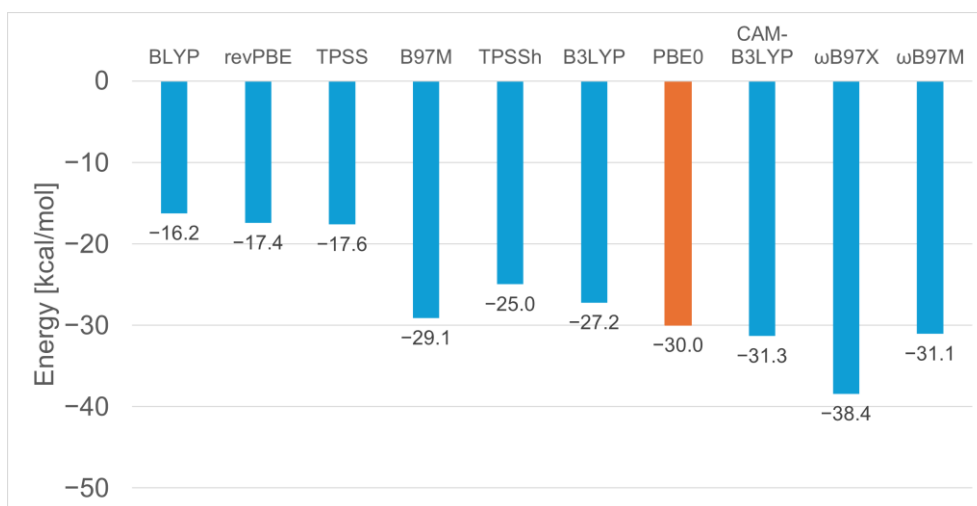
Figure S1. Thermodynamics of hydrogen abstraction reaction: (a) energies (without zero-point energy correction) and (b) Gibbs free energies at 298.15 K.

Section S2. Supplementary figures and tables

Table S1 Potential energies (without zero-point energy correction) plotted in Fig. 2(a). Relative energies (kcal/mol) to the molecules in the ground state.

State	α	β	γ	δ	ε
W10 + PCL–H + $^3O_2$	0.0	0.0	0.0	0.0	0.0
W10* + PCL–H + $^3O_2$	68.7	68.7	68.7	68.7	68.7
H–W10• + PCL• + $^3O_2$	34.3	40.6	40.3	41.1	39.0
H–W10• + PCL–OO•	9.3	4.0	3.8	4.7	3.6
W10 + PCL–OOH	−18.8	−21.0	−19.7	−19.9	−24.8

Table S2 Gibbs free energies (298.15 K) plotted in Fig. 2(b). Relative energies (kcal/mol) to the molecules in the ground state.

Reactions	α	β	γ	δ	ε
W10 + PCL–H + $^3O_2$	0.0	0.0	0.0	0.0	0.0
W10* + PCL–H + $^3O_2$	67.6	67.6	67.6	67.6	67.6
H–W10• + PCL• + $^3O_2$	32.8	37.7	37.5	38.4	36.5
H–W10• + PCL–OO•	22.7	17.5	16.9	18.0	16.7
W10 + PCL–OOH	−4.3	−6.6	−5.8	−5.8	−11.1

Table S3 Potential energies (without the zero-point energy correction) of W10–PCL complex. Relative energies (kcal/mol) to the ground-state complex.[a]

State	α	β	γ	δ	ε
W10 + PCL	17.2	17.2	17.2	17.2	17.2
W10* + PCL	86.0	86.0	86.0	86.0	86.0
HAT reactant	61.5	67.6	(64.1)	(71.3)	67.1
HAT TS[b]	67.0	69.9	(64.5)	(71.4)	72.3
HAT products: C• … HOW	N/A	N/A	(39.8)	42.7	43.7
HAT product: C(=O)O … HOW	33.7	40.2	39.6	40.7	42.7
HAT product: OC=O … HOW	N/A	N/A	N/A	38.9	N/A
H–W10• + PCL•	51.6	57.8	57.5	58.4	56.2
O-insertion TS[c]	61.9	63.3	54.4	61.0	56.2
O-insertion product	46.8	36.2	37.7	38.9	39.6

[a] Values in the parentheses are approximate energies (see text).

[b] Single-point energy after the saddle-point location run.

[c] Maximum of single-point energies on the NEB path.

Table S4 Gibbs free energies (298.15 K) of reactions for PCL hydroperoxides. Unit: kcal/mol.

Reactions	α	β	γ	δ	ε
PCL–OOH → PCL–O• + •OH	28.0	26.3	24.9	26.2	24.3
PCL–OOH + •OH → PCL–OO• + H_2O	−33.5	−36.4	−37.7	−36.7	−32.6
PCL–OOH + H–W10• → PCL–O• + H_2O + W10	−32.5	−34.2	−35.5	−34.2	−36.1
PCL–OOH + •OOH → PCL–O• + H_2O + $^3O_2$	−35.8	−37.5	−38.8	−37.6	−39.5
PCL–OOH + PCL$_\alpha$–OO• → PCL–O• + PCL$_\alpha$–OH + $^3O_2$	−31.3	−33.0	−34.3	−33.0	−34.9
PCL–OOH + PCL$_\beta$–OO• → PCL–O• + PCL$_\beta$–OH + $^3O_2$	−29.4	−31.1	−32.4	−31.1	−33.0
PCL–OOH + PCL$_\gamma$–OO• → PCL–O• + PCL$_\gamma$–OH + $^3O_2$	−29.0	−30.7	−32.0	−30.7	−32.6
PCL–OOH + PCL$_\delta$–OO• → PCL–O• + PCL$_\delta$–OH + $^3O_2$	−28.8	−30.4	−31.8	−30.5	−32.4
PCL–OOH + PCL$_\varepsilon$–OO• → PCL–O• + PCL$_\varepsilon$–OH + $^3O_2$	−33.7	−35.4	−36.7	−35.4	−37.3

**Table S5** Thermochemistry for molecules discussed in the present work. Unit: Hartree.[a]

	E	E + ZPVE	G (298.15 K)
W10 (S_0 min.)	−3728.30569	−3728.18666	−3728.26776
W10 (T_1 min.)	−3728.19615	−3728.07866	−3728.16010
H–W10•			
O_a	−3728.88971	−3728.76192	−3728.84377
O_b	−3728.90487	−3728.77450	−3728.85543
O_c	−3728.89005	−3728.76133	−3728.84238
O_d	−3728.88932	−3728.76028	−3728.84193
O_e	−3728.87649	−3728.74674	−3728.82830
O_f	−3728.89348	−3728.76310	−3728.84372
PCL–H	−770.91793	−770.58556	−770.63317
PCL•			
α	−770.26406	−769.94493	−769.99319
β	−770.25412	−769.93684	−769.98540
γ	−770.25458	−769.93714	−769.98566
δ	−770.25323	−769.93582	−769.98431
ε	−770.25663	−769.93889	−769.98737
PCL–OO•			
α	−920.54070	−920.21161	−920.26195
β	−920.54915	−920.22014	−920.27030
γ	−920.54938	−920.22060	−920.27112
δ	−920.54801	−920.21909	−920.26942
ε	−920.54978	−920.22131	−920.27148
PCL–OOH			
α	−921.18463	−920.84306	−920.89263
β	−921.18807	−920.84688	−920.89637
γ	−921.18609	−920.84515	−920.89501
δ	−921.18640	−920.84532	−920.89498
ε	−921.19422	−920.85366	−920.90356
PCL–O•			
α	−845.42036	−845.09695	−845.14575

β	−845.42676	−845.10329	−845.15218
γ	−845.42691	−845.10379	−845.15294
δ	−845.42585	−845.10230	−845.15087
ε	−845.43638	−845.11351	−845.16248
PCL–OH			
α	−846.09496	−845.75762	−845.80608
β	−846.10051	−845.76289	−845.81135
γ	−846.09981	−845.76286	−845.81157
δ	−846.09916	−845.76147	−845.80949
ε	−846.10822	−845.77094	−845.81938
$^3O_2$	−150.23673	−150.23269	−150.25263
•OH	−75.69388	−75.68538	−75.70231
•OOH	−150.82734	−150.81286	−150.83499
H_2O	−76.39005	−76.36866	−76.38632

[a] E (potential energy), ZPVE (zero-point vibrational energy), and G (Gibbs free energy at 298.15 K).

**Table S6.** Potential energies for HAT reaction at the gamma site in Fig. 4.
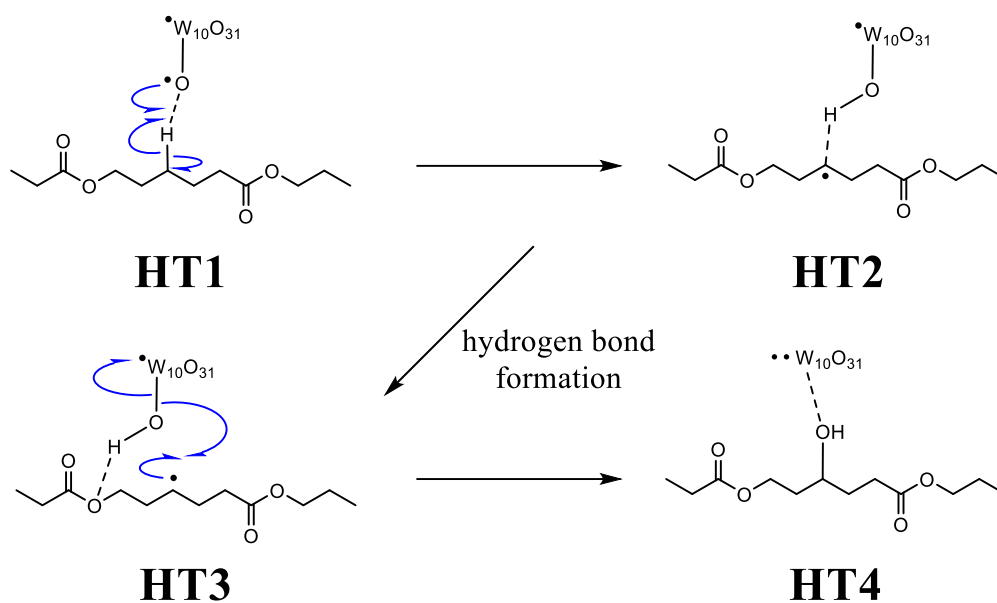
	E [Hartree]	$< S^2 >$	ΔE [kcal/mol]
[W10 … PCL–H] (ground-state min.)	−4499.25109	0.000	0.00
HT1	−4499.14898	2.016	64.08
HT2	−4499.18765	2.016	39.81
HT3	−4499.18794	2.017	39.63
Max (**HT3 → HT4**)[a]	−4499.16446	2.020	54.36
HT4	−4499.19109	2.021	37.65

[a] Energy maximum on the NEB path.

**Table S7.** Potential energies for reoxidation of HAT product complex in Fig. 5.
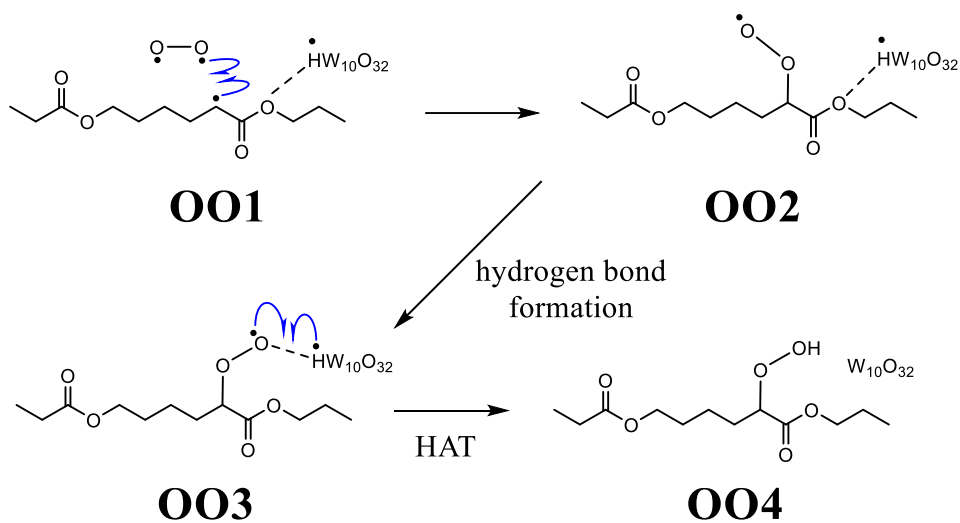
|	E [Hartree]	$< S^2 >$	ΔE [kcal/mol]
[W10 … PCL–H] + $^3O_2$ (ground-state min.)	−4649.48782	0.000/2.010	0.00
[H–W10• … PCL•] + $^3O_2$ (infinite separation)	−4649.43405	2.016/2.010	33.74
OO1	−4649.43734	2.028[b]	31.68
Max (**OO1** → **OO2**)[a]	−4649.42553	1.814[b]	39.09
OO2	−4649.47280	1.016[c]	9.43
OO3	−4649.46325	1.016[c]	15.42
Max (**OO3** → **OO4**)[a]	−4649.45498	1.006[c]	20.61
OO4	−4649.50926	0.000	−13.45

[a] Energy maximum from the relaxed surface scan.

[b] Open-shell singlet state of [H–W10 (↑) PCL (↑)] … $^3O_2$ (↓↓).

[c] Open-shell singlet state of [H–W10 (↑) PCL–OO (↓)].

Table S8. Potential energies for SET in Fig. 6.
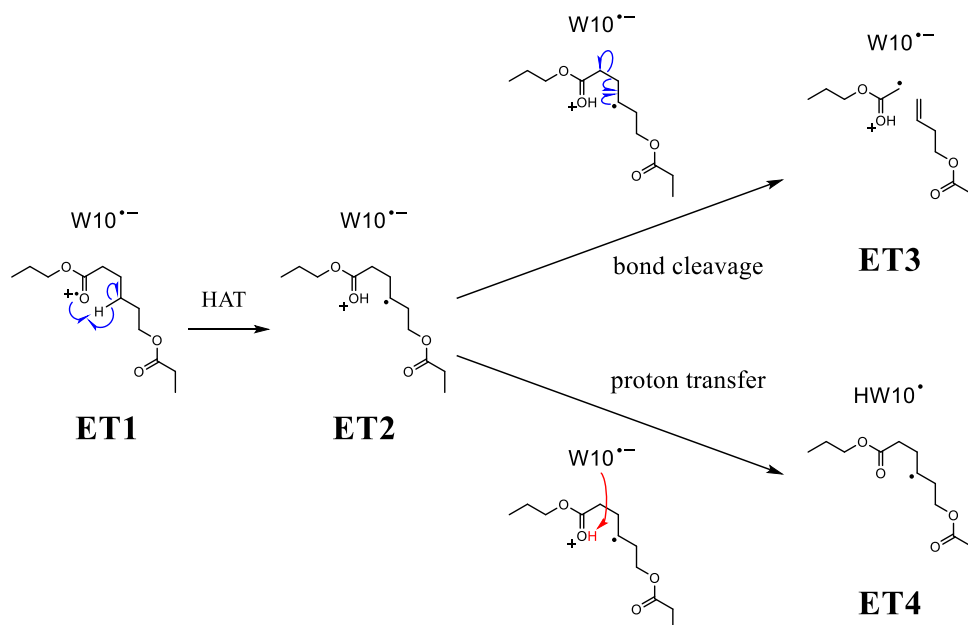
	E [Hartree]	$< S^2 >$	ΔE [kcal/mol]
[W10…PCL–H] (ground-state min.)	−4499.25109	0.00	0.00
ET1	−4499.14523	2.017	66.43
ET2	−4499.18124	2.016	43.83
ET3	−4499.15079	2.018	62.94
Max (**ET2 → ET4**)	−4499.17630	2.016	46.93
ET4	−4499.18208	2.016	43.30
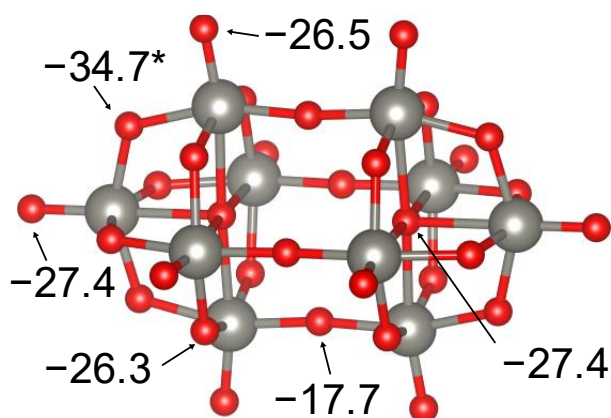
Figure S2. Gibbs free energies (298.15 K) of the α-hydrogen abstraction: W10* + PCL–H$_\alpha$ → H–W10• + PCL$_\alpha$•. The bridge oxygen site (asterisk) is most reactive. Unit: kcal/mol.
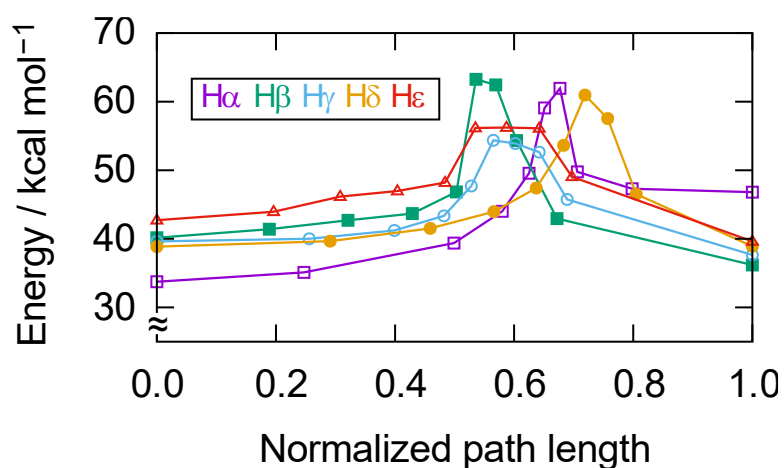
Figure S3. Single point energies on the NEB paths for the O-insertion reaction. Relative energies (kcal/mol) to the ground-state complex.
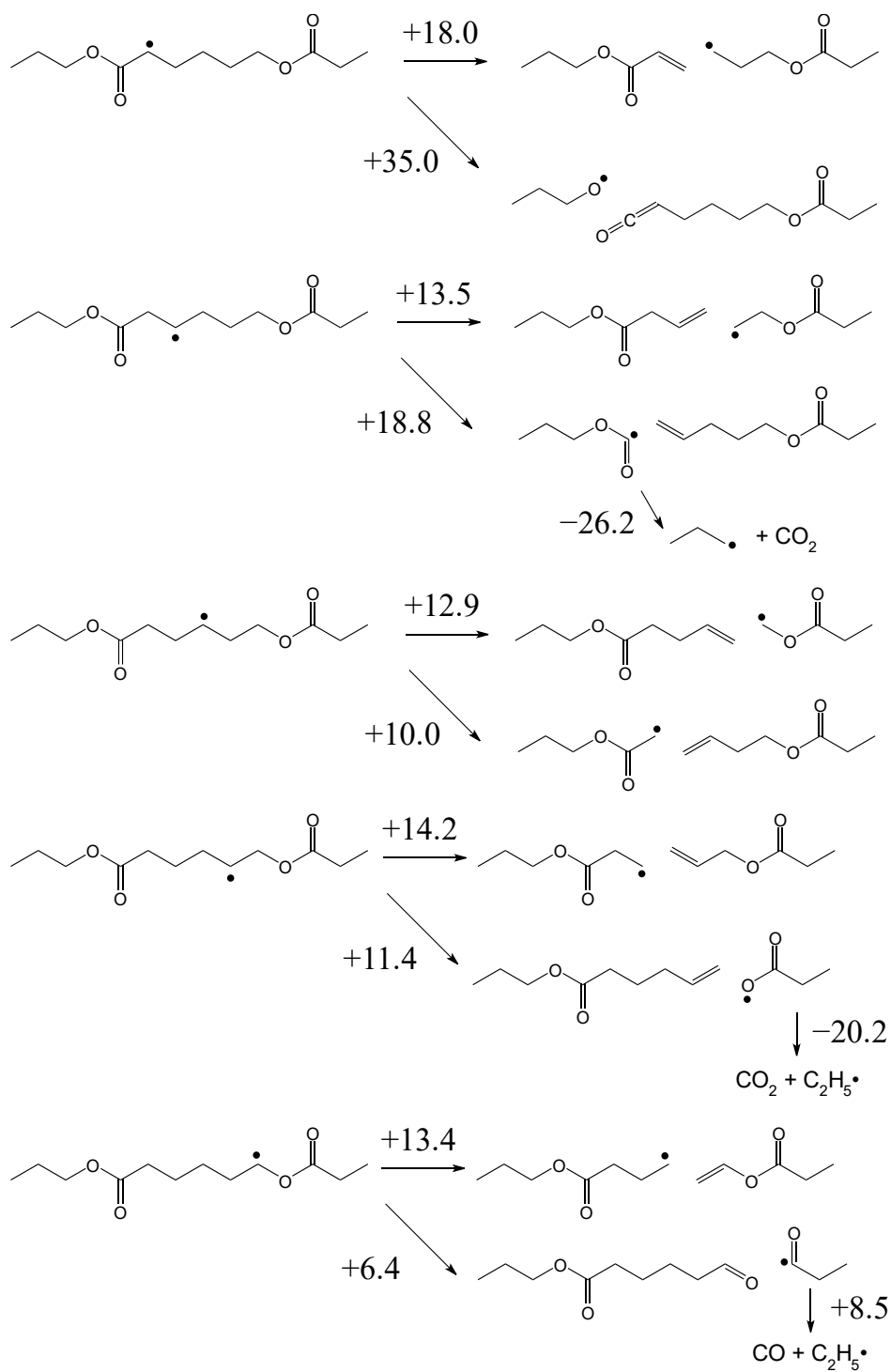
Figure S4. Gibbs free energies (298.15 K) of β-cleavage for PCL• radicals. Unit: kcal/mol.
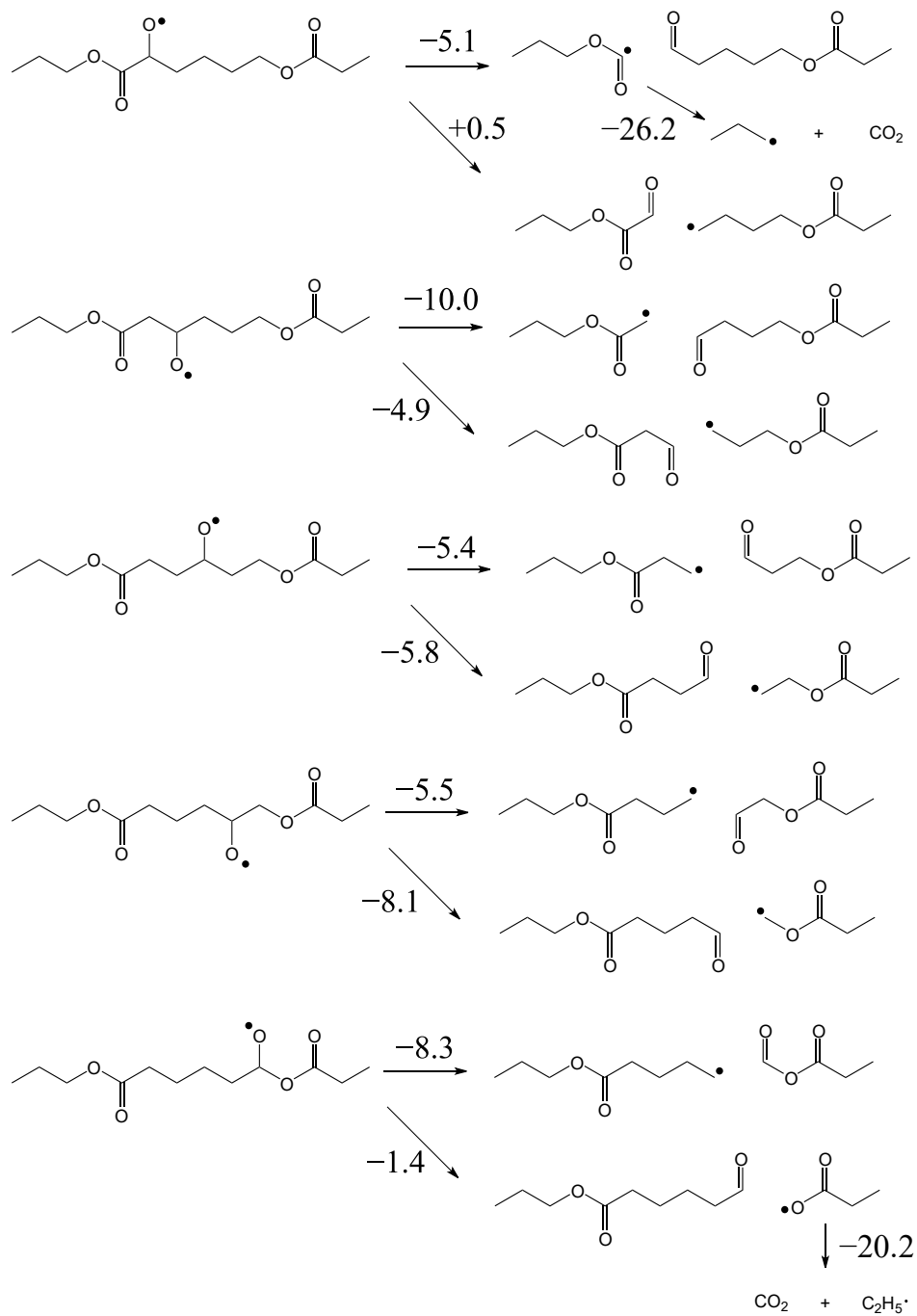
Figure S5. Gibbs free energies (298.15 K) of β-cleavage for PCL–O• radicals. Unit: kcal/mol.

References

1. Y. Zhang and W. Yang, Comment on "Generalized Gradient Approximation Made Simple," *Phys. Rev. Lett.*, 1998, **80**, 890–890.

2. J. Tao, J. P. Perdew, V. N. Staroverov and G. E. Scuseria, Climbing the Density Functional Ladder: Nonempirical Meta–Generalized Gradient Approximation Designed for Molecules and Solids, *Phys. Rev. Lett.*, 2003, **91**, 146401.

3. J. P. Perdew, J. Tao, V. N. Staroverov and G. E. Scuseria, Meta-generalized gradient approximation: Explanation of a realistic nonempirical density functional, *J. Chem. Phys.*, 2004, **120**, 6898–6911.

4. V. N. Staroverov, G. E. Scuseria, J. Tao and J. P. Perdew, Comparative assessment of a new nonempirical density functional: Molecules and hydrogen-bonded complexes, *J. Chem. Phys.*, 2003, **119**, 12129–12137. erratum: *ibid.,* 2004, **121**, 11507.

5. C. Adamo and V. Barone, Toward reliable density functional methods without adjustable parameters: The PBE0 model, *J. Chem. Phys.*, 1999, **110**, 6158-6170.

6. A. Najibi and L. Goerigk, The Nonlocal Kernel in van der Waals Density Functionals as an Additive Correction: An Extensive Analysis with Special Emphasis on the B97M-V and ωB97M-V Approaches, *J. Chem. Theory Comput.*, 2018, **14**, 5725–5738.

7. N. Mardirossian and M. Head-Gordon, Mapping the genome of meta-generalized gradient approximation density functionals: The search for B97M-V, *J. Chem. Phys.*, 2015, **142**, 074111.

8. N. Mardirossian and M. Head-Gordon, ωB97X-V: A 10-parameter, range-separated hybrid, generalized gradient approximation density functional with nonlocal correlation, designed by a survival-of-the-fittest strategy, *Phys. Chem. Chem. Phys.* 2014, **16**, 9904–9924.

9. N. Mardirossian and M. Head-Gordon, ωB97M-V: A combinatorially optimized, range-separated hybrid, meta-GGA density functional with VV10 nonlocal correlation, *J. Chem. Phys.*, 2016, **144**, 214110.

10. S. Grimme, J. Antony, S. Ehrlich and H. Krieg, A consistent and accurate ab initio parametrization of density functional dispersion correction (DFT-D) for the 94 elements H-Pu, *J. Chem. Phys.*, 2010, **132**, 154104.

11. S. Grimme, S. Ehrlich and L. Goerigk, Effect of the damping function in dispersion corrected density functional theory, *J. Comput. Chem.*, 2011, **32**, 1456–1465.

12. F. Neese, F. Wennmohs, U. Becker and C. Riplinger, The ORCA quantum chemistry program package, *J. Chem. Phys.*, 2020, **152**, 224108.

13. N. Mardirossian and M. Head-Gordon, Thirty years of density functional theory in computational chemistry: an overview and extensive assessment of 200 density functionals, *Mol. Phys.*, 2017, **115**, 2315–2372.